Available online at www.sciencedirect.com
SCIENCE DIRECT
Polymer 47 (2006) 480–488
polymer
www.elsevier.com/locate/polymer

# Low percolation thresholds of electrical conductivity and rheology in poly(ethylene terephthalate) through the networks of multi-walled carbon nanotubes

Guangjun Hu, Chungui Zhao, Shimin Zhang, Mingshu Yang *, Zhigang Wang *

*Key Laboratory of Engineering Plastics, Joint Laboratory of Polymer Science and Materials, Institute of Chemistry, Chinese Academy of Sciences, Beijing 100080, People's Republic of China*

Received 7 August 2005; received in revised form 31 October 2005; accepted 13 November 2005
Available online 28 November 2005

**Abstract**

Coagulation method was first used to prepare nanocomposites of multi-wall carbon nanotubes (MWNT) and poly(ethylene terephthalate) (PET). The morphology of nanocomposites is characterized using transmission electronic microscopy and scanning electronic microscopy. A coating on MWNT by PET chains is observed by comparison of micrographs of purified MWNT and MWNT encapsulated by PET chains in the nanocomposites, and this coating is considered as evidence of interfacial interaction between MWNT and PET chains. Both electrical conductivity and rheological properties have been well characterized. With increasing MWNT loading, the nanocomposites undergo transition from electrically insulative to conductive at room temperature, while the melts show transition from liquid-like to solid-like viscoelasticity. The percolation threshold of 0.6 wt% (based on viscosity) for rheological property and 0.9 wt% for electrical conductivity has been found. The low percolation threshold results from homogeneous dispersion of MWNT in PET matrix and high aspect ratio of MWNT. The less rheological percolation threshold than electrical percolation threshold is mainly attributed to the fact that a denser MWNT network is required for electrical conductivity, while a less dense MWNT network sufficiently impedes PET chain mobility related to the rheological percolation threshold.


*Keywords:* Nanocomposite; Multi-wall carbon nanotubes; Poly(ethylene terephthalate)

## 1. Introduction

Since discovered in 1990s [1], carbon nanotubes (CNT), including single-wall carbon nanotube (SWNT) and multi-wall carbon nanotubes (MWNT), have attracted great interests throughout the academic and industrial world. CNT possess extraordinary electrical, mechanical and thermal properties: elastic modulus is up to 1 TPa, thermal conductivity may be twice as high as that of diamond and electric-current-carrying ability may be 1000 times as that of copper wires [2]. Their high aspect ratio makes them possible to possess percolation threshold at low CNT loading in nanocomposites. CNT have potential applications in many areas such as biosensors, conducting agent, field-effect transistor, and nanocomposites.

In order to achieve superior performance in CNT filled polymer nanocomposites, there are two key issues to be stressed: dispersion of CNT in polymer matrix and interaction between CNT and polymer. Currently, melt mixing compounding [3–14], curing/in situ polymerization [15–23] and coagulation [24–28] are usually used to prepare these kinds of nanocomposites. Kharchenko et al. [3] reported that both electrical conductivity and viscosity of polypropylene/MWNT nanocomposites decreased strongly with increasing shear rate, and these nanocomposites exhibited large and negative normal stress. Nogales et al. [15] applied in situ polycondensation reaction to prepare PBT/SWNT nanocomposites and achieved electrical percolation threshold as low as 0.2 wt% of SWNT loading. Du et al. [20,21] prepared poly(methyl methacrylate)/SWNT nanocomposites via coagulation method, and employed optical microscopy, Raman imaging and SEM to determine dispersion of nanotubes at different length scales. They observed that rheological percolation threshold was smaller than that of electrical conductivity, and attributed this difference to smaller inter-tube distance required for electrical conductivity as compared to that for impeding polymer chain mobility.

* Corresponding authors. Tel./fax: +86 10 82615665.
*E-mail addresses:* yms@iccas.ac.cn (M. Yang), zgwang@iccas.ac.cn (Z. Wang).

0032-3861/$ - see front matter © 2005 Elsevier Ltd. All rights reserved.
doi:10.1016/j.polymer.2005.11.028

CNT filled polyethylene [2,11], polypropylene [3–6], polyamide [7–10], polystyrene [16], poly(methyl methacrylate) [20,21] and many other polymers [23–28] are reported recently, whereas, there is little literature covering CNT filled poly(ethylene terephthalate) (PET) nanocomposites to our knowledge. Wu et al. [29] prepared CNT filled PET/poly(vinylidiene fluoride) blend via injection molding, and the results showed an onset of electrical conductivity at CNT loadings of 3–5 wt%. Saran et al. [30] immersed PET film into SWNT dispersion, and obtained thin, strongly adherent films of SWNT bundles on PET, which showed low sheet resistance, optical transparency and robust flexibility. According to literature, electrical and rheological properties of CNT filled PET nanocomposites are still unclear. In this study, we first used coagulation method to prepare PET/MWNT nanocomposites by dispersing MWNT into the mixture of common solvents for both MWNT and PET. The dispersion of MWNT in PET matrix, and the percolation thresholds of electrical conductivity and rheological properties of the nanocomposites have been systematically investigated.

## 2. Experimental

### 2.1. Materials and preparation of PET/MWNT nanocomposites

Pristine MWNT with diameter 10–20 nm and length 5–15 μm were obtained from Shenzhen Nanotech Port Co., Ltd (Shenzhen, China). Commercial grade PET was kindly provided by Yizheng Chemical Fibre Co., Ltd (Yizheng, China). The intrinsic viscosity of PET measured in phenol-1,1,2,2-tetrachloroethane (3:2 by mass) as 0.64 dL/g, and the corresponding viscosity molecular weight was 50 kg/mol.

MWNT were purified by air oxidation [31,32] to remove amorphous carbons and residual metal catalysts as followed: pristine MWNT were first exposed to 500 °C in air for 1 h, and then exposed to concentrated hydrochloric acid. The productivity was 78%.

Quantitative MWNT were added to ODCB–phenol (1:1 by mass) and ultrasonicated (40 KHz, 100 W) for 6 h to obtain uniformly dispersed MWNT suspension and then PET was added in. The mixture was stirred at 110 °C. After PET was dissolved, the solution was precipitated in extensive methanol in ventilating cabinet. The sediment was rinsed with massive methanol before drying under vacuum at 110 °C to obtain PET/MWNT nanocomposites. It is noted here that the mean length of MWNT as received is 5–15 μm, and no much difference before and after ultrasonication has been observed.

### 2.2. Electron microscopic characterization

Transmission electron microscopy (TEM) observation of the pristine and purified MWNT was performed on a JEOL JEM-2010 operated at 200 kV. TEM observation of the morphology of the PET/MWNT nanocomposites was carried on Hitachi (Japan) H-800 with an acceleration voltage of 200 kV. The ultrathin slices of the nanocomposites were prepared by sectioning the sample under cryogenic condition.

Scanning electron microscopy (SEM) observation was conducted with JEOL S-4300 operated at 15 kV. The specimens were quenched and fractured in liquid nitrogen. Half samples were etched in potassium hydroxide solution in ethanol to eliminate amorphous PET on the surface. The fracture surfaces were coated with platinum utilizing GIKO IB-3 ion coater.

SEM and TEM micrographs were analyzed using image analysis software Scion Image 4.02 Beta version (Scion, USA).

### 2.3. Electrical conductivity analysis

Circular plates with 2.5 mm in diameter and 1.4 mm in thickness upon circular aluminum electrodes were obtained by compression molding at 280 °C for 5 min. Strong adhesion enables fine contact between aluminum and PET. The current–voltage ($I$–$U$) behavior was tested with the apparatus named HEWLETT PACKARD (HP) 4140B picoammeters/DC voltage at room temperature. Two test fixtures were chosen. High resistance test fixture was used to measure samples with the MWNT loadings up to 0.5 wt%. The semiconductor test fixture was used to measure samples with higher MWNT loadings. By applying suitable voltages ($U$) with appropriate gaps, the corresponding electrical currents ($I$) were recorded. The resistance $R$ is calculated from the $I$–$U$ curves according to Ohm's law. Based on the resistance $R$, the electrical conductivity $\sigma$, can be calculated by using Eq. (1)

$$\sigma = \frac{1}{\rho} = \frac{d}{RS} = \frac{dI}{SU} \tag{1}$$

where $\rho$ is electrical resistivity, $d$ is thickness of the sample between two electrodes, and $S$ is cross-sectional area perpendicular to current direction in specimen.

### 2.4. Rheological measurements

Prior to rheological measurements, compression molded bars of about $20 \times 10 \times 2$ mm$^3$ were annealed under vacuum at 110 °C for 12 h to completely remove the moisture. Dynamic shear rheological measurements were carried out on Rheometrics SR200 dynamic stress rheometer at 265 °C in nitrogen atmosphere and run with 25 mm parallel-plate geometry and 1 mm sample gap. The dynamic viscoelastic properties were determined using low strain values (0.05–5%) with frequency from 0.1 to 500 rad/s, which were shown within the linear viscoelastic region for these materials.

### 2.5. Glass transition temperature ($T_g$) measurements

$T_g$ was determined using differential scanning calorimetry (DSC) (Perkin–Elmer DSC 7) with heating rate of 20 °C/min under nitrogen atmosphere. Samples were first heated to 280 °C at a ramp of 20 °C/min and kept for 3 min, and then cooled to 25 °C at the ramp of 20 °C/min to eliminate thermal history prior to measuring $T_g$.

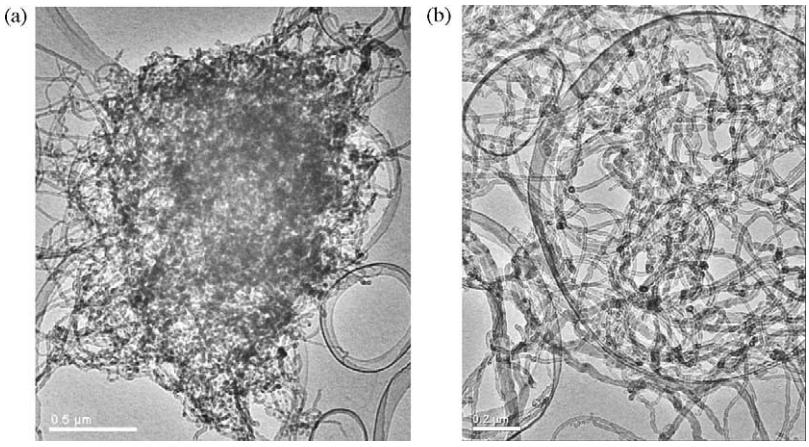


Fig. 1. TEM micrographs, showing morphologies of pristine MWNT (a) and purified MWNT (b). The scale bars correspond to 500 nm in (a) and 200 nm in (b).

## 3. Results and discussion

### 3.1. Morphology and dispersion of MWNT

Due to possible π–π conjugation and formation of a sonopolymer, SWNT has been reported to form stable dispersion in ODCB under ultrasonication [33,34]. The present work shows that MWNT can also be dispersed well in ODCB–phenol (1:1 by mass) mixture. In fact, the dispersion of MWNT in ODCB–phenol mixture is stable for several weeks. As compared in Fig. 1 of the morphologies by TEM observation, dense coils and impurities are found in pristine MWNT (Fig. 1(a)); whereas, much less impurities are found in purified MWNT (Fig. 1(b)) and MWNT are much less entangled. The black dots in Fig. 1(b) are actually opening ends of MWNT, which means there are reactive dangling bonds, and FT-IR spectrum shows the existence of carboxyl group. Because ODCB–phenol mixture is one of the good solvent mixtures for PET, MWNT dispersed ODCB–phenol solution was successfully used to prepare PET/MWNT nanocomposites in the present work.

In Fig. 2, TEM micrographs of cryo-microtomed PET/MWNT nanocomposites for two different MWNT loadings of 0.5 and 4.8 wt% are displayed. As would be discussed later, the electrical percolation threshold of PET/MWNT nanocomposites is about 0.9 wt%. These two MWNT loadings are deliberately chosen to reveal the obvious difference before and after formation of MWNT networks throughout PET matrix. TEM observation reveals a homogeneous dispersion of MWNT in PET matrix. As shown in Fig. 2(a) and (b), MWNT are randomly dispersed without preferred alignments. The random MWNT network penetrating into PET matrix is shown in Fig. 2(b). MWNT remain curved or even interwoven throughout PET matrix. Most of MWNT embedded into the matrix show some degree of waviness or entanglements along axial direction. Such curvature probably reduces the efficient structural reinforcements in comparison to the theoretical promises [35]. In addition, MWNT network is more clearly shown by SEM observation. Fig. 3(a) shows SEM micrograph of the unetched cryo-fractured surface of PET/MWNT nanocomposite with MWNT loading of 9.0 wt%, indicating clear nanotube network penetrating throughout PET matrix. Fig. 3(b) shows SEM micrograph of the etched surface, and much clear nanotube network is revealed.

In order to quantitatively demonstrate the fact that MWNT are actually encapsulated by PET, Scion Image software

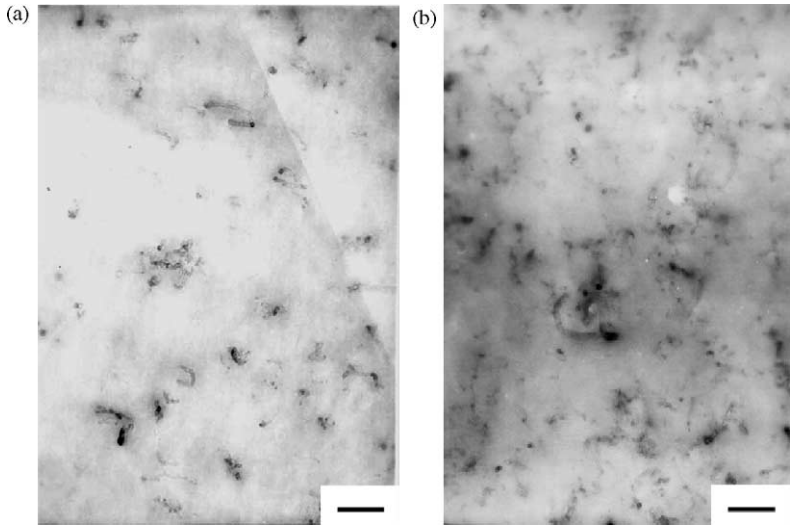


Fig. 2. TEM micrographs of cryo-microtomed nanocomposites for different MWNT loadings, *m*: (a) 0.5 wt% and (b) 4.8 wt%. The scale bar is 250 nm.

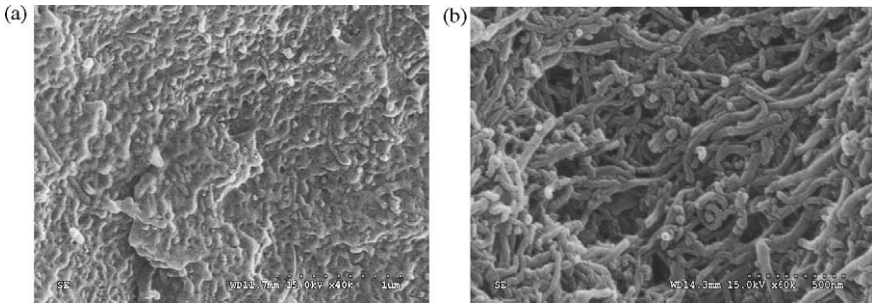


Fig. 3. SEM micrographs of PET/MWNT nanocomposite with MWNT loading of 9.0 wt%, showing a network of MWNT penetrating into PET matrix, (a) unetched and (b) etched.

was used to determine the diameters of purified MWNT (from Fig. 1(b)), unetched MWNT encapsulated by PET (from Fig. 3(a)) and etched MWNT encapsulated by PET (from Fig. 3(b)). The average diameter is 16 nm for purified MWNT, 50 nm for unetched MWNT encapsulated by PET and 34 nm for etched MWNT encapsulated by PET. The average diameter of MWNT in the nanocomposites (50 nm) is about three times of that of purified MWNT (16 nm). This reveals that PET encapsulates MWNT, and interfacial interaction exists between MWNT and PET. The driving attractive force behind this interfacial interaction might be possible π–π conjugation between PET chains and MWNT due to their common aromatic chemical structures and also esterification between hydroxyl group at the end of PET chains and carboxyl group at MWNT defects. The exact mechanism of how MWNT interact with PET is still unclear and under further investigation. Furthermore, because etching in potassium hydroxide in ethanol assumed mostly amorphous phase of PET on the fractured surface, the remained encapsulation part of PET was highly crystalline.

### 3.2. Electrical conductivity properties

As shown in Fig. 4, the current–voltage (*I–U*) curves of the PET/MWNT nanocomposites show good linearity, disclosing that the curves observe the Ohm's law quite well. The little curvature on the curves at MWNT loadings of 0 and 0.5 wt% is attributed to the accumulated charges during manual settings of the employed voltages. The electric resistance of the nanocomposites is equal to the reciprocal of the slope of the curves. The electrical conductivity ($\sigma$) of the nanocomposites is calculated according to Eq. (1), and it is presented in Fig. 5 as a function of the MWNT loading. Pure PET is excellent insulating material with electrical conductivity of $8.6\times10^{-17}$ S/cm. The nanocomposites exhibit an abrupt increase in 8 orders of magnitude for MWNT loadings from 0.5 to 1 wt%. This can be regarded as the formation of a percolative path of the conducting network throughout PET matrix. At MWNT loadings exceeding 2.0 wt%, the electrical conductivity increases slowly with increasing MWNT loading, and approximates to a value of $1\times10^{-4}$ S/cm.

According to the classical percolation theory, electrical conductivity of a filled material follows a power law relationship as shown in Eq. (2):

$$\sigma \propto (m - m_{c,\sigma})^{\beta_{c,\sigma}} \tag{2}$$

where $m$ is the volume fraction of the filler, $m_{c,\sigma}$ is the volume fraction of percolation threshold, and $\beta_{c,\sigma}$ is the critical exponent, which is related to the system dimension. In current case, because the density of nanotubes can only be appropriately estimated (1.4–1.9 g/cm$^3$), mass fraction of MWNT is preferred

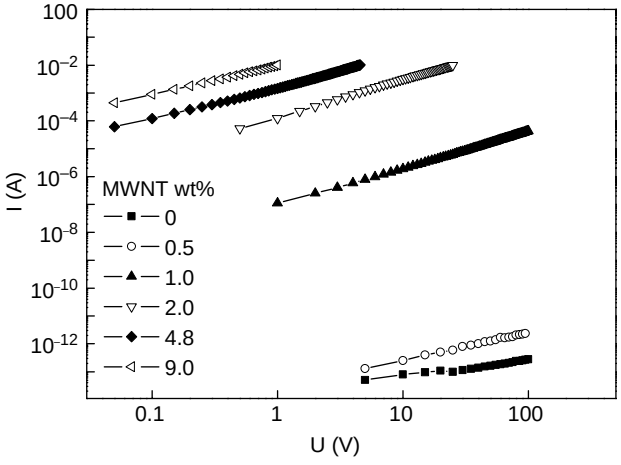


Fig. 4. Log–log *I–U* plot of PET/MWNT nanocomposites with different MWNT loadings measured at room temperature.

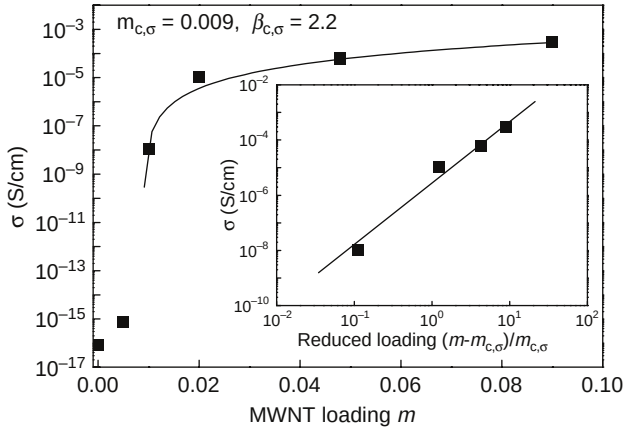


Fig. 5. Electrical conductivity ($\sigma$) of the PET/MWNT nanocomposites as a function of MWNT loading. Inset: a log–log plot of electrical conductivity versus reduced MWNT loading. The solid lines are fits to a power law dependence of electrical conductivity on the reduced MWNT loading (Eq. (2)).

instead of volume fraction. Critical exponent ($\beta_{c,\sigma}$) by theoretical prediction ranges from 1.6 to 2.0 for three-dimensional (3D) percolating systems [36], while experimental values between 0.7 and 3.1 have been reported for the CNT-filled nanocomposites [16–19]. As shown in Fig. 5, the electrical conductivity of PET/MWNT nanocomposites agrees well with the percolation behavior given by Eq. (2). The best fitting to the experimental values resulted in $m_{c,\sigma}$ of 0.009 and $\beta_{c,\sigma}$ of 2.2. The critical exponent of the nanocomposite system is in accordance with theoretical expectation and experimental observation, hinting formation of 3D percolating network at 0.9 wt%. Thus, the fitting result indicates a low percolation threshold at MWNT loading of 0.9 wt%. Measurement of the average aspect ratio of these MWNT from TEM micrographs presents the value of ca. 150, comparable to the order of magnitude estimated from the geometrical percolation threshold [3]. This result is consistent to Garboczi's report. Garboczi et al. pointed out that the percolation threshold for overlapping needles with an aspect-ratio range between 100 and 1,000 is in the range of 0.1–1% [37].

The electrical percolation thresholds for CNT-filled nanocomposites with thermosets such as epoxy resin [17,18] and polyimide [19] usually lie in the range from 0.1 to 1 wt%, while the values for thermoplastics such as polyethylene [2], polypropylene [3,4], polyamide [10], polycarbonate [12], and polystyrene [16] lie between 0.2 and 15 wt%. Bin et al. [2] prepared MWNT/high-density polyethylene by gelation/crystallization from solutions, and revealed that the percolation occurred between 5 and 15 wt%. Kharchenko et al. [3] prepared polypropylene/MWNT nanocomposites by melt blending, and displayed that the percolation thresholds for conductivity and firmness were both at the concentration ranging from 0.25 to 1 wt% at 200 °C. Meincke et al. [10] found that CNT-filled polyamide-6 showed an onset of electrical conductivity at CNT loadings of 4–6 wt%. Nogales et al. [15] prepared SWNT filled poly(butylene terephthalate) by in situ polymerization and reported achievement of low percolation threshold around 0.2 wt% of SWNT. Du et al. [20,21] used coagulation method to produce SWNT/poly(methyl methacrylate) (PMMA) nanocomposites, and disclosed percolation threshold between 0.2 and 2 wt%.

The percolation threshold value of 0.9 wt% measured at room temperature in the present work is one of the lowest values of ambient temperature electrical conductivity percolation threshold reported in MWNT nanocomposites with thermoplastics. The low percolation threshold is attributed to high aspect ratio of MWNT and homogenous dispersion of MWNT in PET matrix, which was confirmed in morphology characterization. It is noticed that at 1 wt% MWNT loading, the conductivity level exceeds the antistatic criterion of thin films ($1\times10^{-8}$ S/cm), which is one of the targeted applications for the PET/MWNT nanocomposites.

### 3.3. Rheological properties

The melt viscosity ($\eta$) of PET/MWNT nanocomposites versus frequency ($\omega$) is shown in Fig. 6. The viscosity of neat PET is almost independent of frequency, and

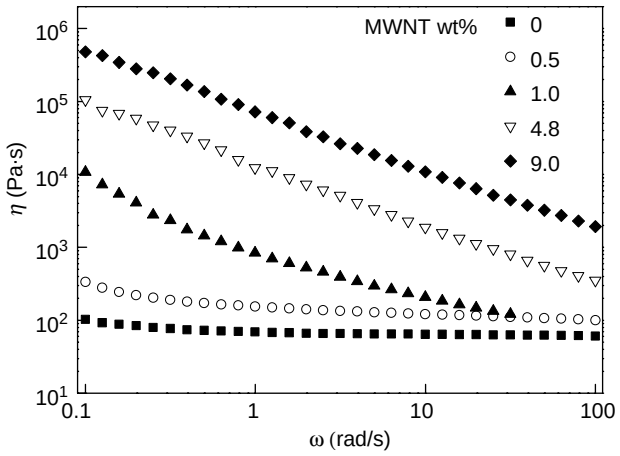


Fig. 6. Viscosity ($\eta$) of PET/MWNT nanocomposites versus frequency ($\omega$) at 265 °C.

the nanocomposite at MWNT loading of 0.5 wt% shows a weak shear thinning behavior. Both curves of PET and nanocomposite at MWNT loading of 0.5 wt% show Newtonian plateaus within the studied frequency range. However, the nanocomposites containing higher MWNT loadings exhibit strong shear thinning behavior, and the viscosities are orders of magnitude higher than that of neat PET at low frequency. For the sample containing 1 wt% MWNT, the viscosity curve displays a steep slope at low frequency, and the Newtonian plateau disappears. For the samples with even higher loadings of MWNT, the viscosity curves are nearly linear throughout the studied range of frequency. Overall, the viscosity increases with increasing MWNT loading. The effect of MWNT is more pronounced at low frequency and such effect weakens with increasing frequency due to shear thinning effect. Above results are in good agreement with both theoretical predictions [38] and experimental observations [3,4] for the fibre-reinforced polymer systems.

The increase in viscosity is caused by similar increase in storage modulus ($G'$, Fig. 7) and loss modulus ($G''$, Fig. 8). The power law dependence of $G'$ and $G''$ on frequency is listed in

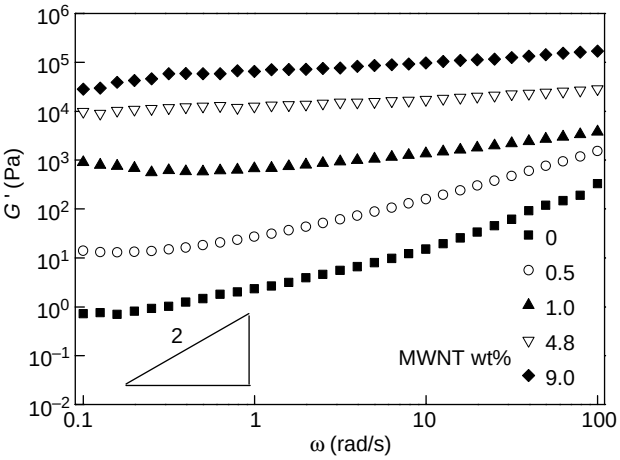


Fig. 7. Storage modulus ($G'$) of PET/MWNT nanocomposites versus frequency ($\omega$) at 265 °C.

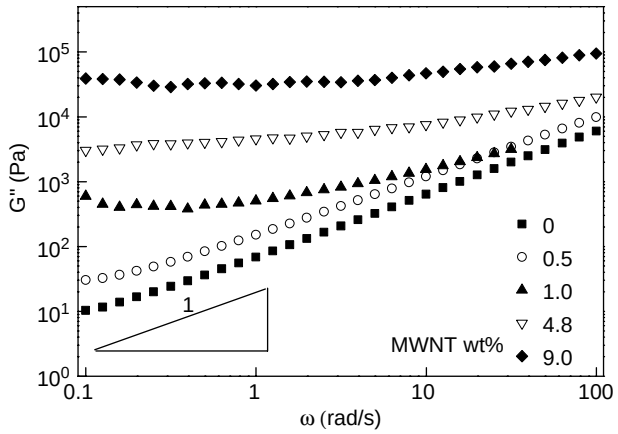


Fig. 8. Loss modulus ($G''$) of PET/MWNT nanocomposites versus frequency ($\omega$) at 265 °C.

Table 1. Values of 2 for $G' \propto \omega^2$ and 1 for $G'' \propto \omega^1$ are expected for the noncrosslinked linear polymer melts, but large deviations occur, especially when network structures are formed in molten state. At molten state, in the case of pure PET, polymer chains exhibit terminal behavior like linear polymers with scaling properties of approximately $G' \propto \omega^{1.2}$ and $G'' \propto \omega^{0.9}$. When the MWNT loading exceeds 0.5 wt%, the terminal behavior disappears, and the dependence of $G'$ and $G''$ on $\omega$ weakens. The effect of MWNT on the rheological behavior of the nanocomposites is strong throughout the frequencies. This nonterminal behavior suggests that MWNT not only cause the restriction of PET chain relaxation but also influence the short-range dynamics or local motion of the PET chains in the nanocomposites. This performance can be attributed to existence of MWNT networks, and to the possible π–π conjugation between PET chains and MWNT as mentioned earlier. The restriction of PET chains by MWNT is also confirmed by $T_g$ measurements (Table 1). Addition of MWNT into PET matrix causes increases in $T_g$ as predicted. In order to figure out the reason of abnormal decrease in $T_g$ at MWNT loading of 0.5 wt%, $T_g$ measurements of PET/MWNT nanocomposites prepared through melt mixing by DMA are conducted, which show consistent increase in $T_g$ with increasing of MWNT loading. It suggests that MWNT may absorb some solvents onto the surface due to large surface areas and possible π–π conjugation with ODCB–phenol, and it is difficult to eliminate the solvent residues thoroughly. The solvent residues cause the decrease in $T_g$ at low MWNT loading. Whereas, at high MWNT loadings, the constraint effect caused by MWNT overwhelms the plastifying effect of solvent residues, resulting in increasing of $T_g$.

Table 1
Slopes of $G'$ versus $\omega$ and of $G''$ versus $\omega$ for PET/MWNT nanocomposites

| MWNT loading (%) | Slope of $G'$ versus $\omega$ | Slope of $G''$ versus $\omega$ | $T_g$ (°C) |
|---|---|---|---|
| 0 | 1.23 | 0.92 | 80.9 |
| 0.5 | 1.21 | 0.84 | 78.5 |
| 1.0 | 0.42 | 0.28 | 81.1 |
| 4.8 | 0.21 | 0.19 | 87.0 |
| 9.0 | 0.23 | 0.05 | 87.6 |
| Linear polymer | 2 | 1 | – |

The power law dependence of $G'$ and $G''$ on frequency weakens monotonically with increasing MWNT loading, from $\omega^{1.2}$ to $\omega^{0.2}$ and $\omega^{0.9}$ to $\omega^{0.05}$, respectively. Both $G'$ and $G''$ become nearly independent of frequency as MWNT loading ranges from 0.5 to 1 wt%. This is an indicator to transition from liquid-like to solid-like viscoelastic behaviors. The nonterminal behavior in the nanocomposites should be caused by formation of nanotube network, which confines long-range motions of PET chains. As shown previously in TEM and SEM micrographs, MWNT network does exist, where nanotubes randomly intersect each other and form disordered reticular structure. The viscoelastic changing from typical linear terminal behavior to nonterminal behavior has also been conformed in various types of polymer nanocomposites including polymer/CNT [3,4] and polymer/clay [39] systems.

The viscosities of PET/MWNT nanocomposites versus MWNT loading at different frequency are shown in Fig. 9. At low frequencies (0.1 and 1.0 rad/s), the viscosity curves show steep slopes between 0.5 and 1.0 wt% of MWNT loadings, and this implies the obvious changes of the microstructures in the samples. At high frequencies (10 and 31.5 rad/s), the viscosity shows almost linear increase with MWNT loading.

The viscosity at 0.1 rad/s shows typical percolation behavior. In Fig. 7, it is seen that the storage modulus at low frequency also experiences sharp increase between 0 and 1 wt% of MWNT loadings, which could also be considered as typical percolating behavior. And this sharp increase in storage modulus is related to formation of MWNT networks interpenetrating into PET molecular chains. To determine the rheological thresholds of PET/MWNT nanocomposites, two modified power law relations are drawn as following equations:

$$\eta \propto (m - m_{c,\eta})^{\beta_{c,\eta}} \tag{3}$$

$$G' \propto (m - m_{c,G'})^{\beta_{c,G'}} \tag{4}$$

where $\eta$ is viscosity, $G'$ is storage modulus, $m$ is MWNT loading, $m_{c,\eta}$ and $m_{c,G'}$ are rheological percolation thresholds, and $\beta_{c,\eta}$ and $\beta_{c,G'}$ are critical exponents. The best fitting for

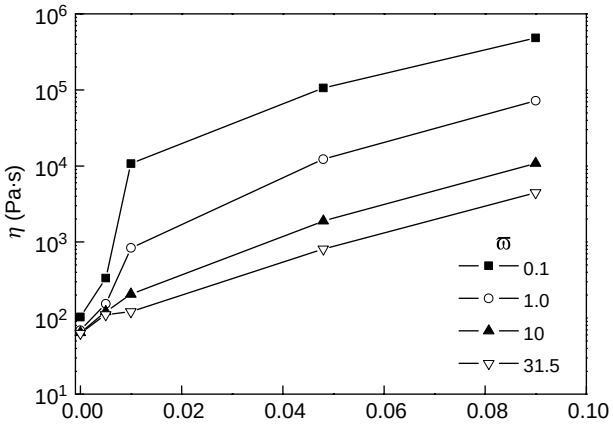


Fig. 9. Viscosity ($\eta$) versus MWNT loading at different frequency.

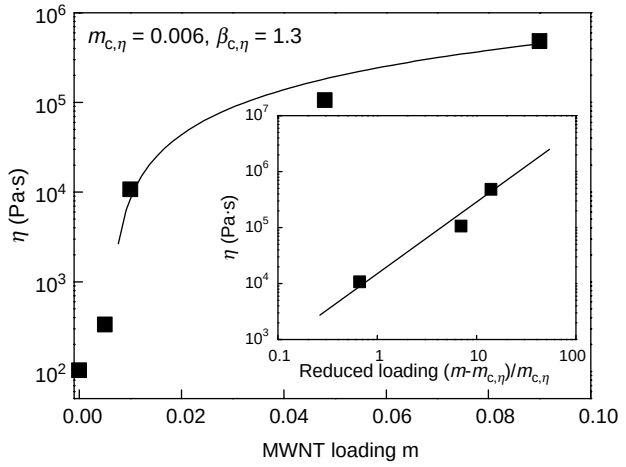


Fig. 10. Viscosity ($\eta$) of PET/MWNT nanocomposites as a function of MWNT loading at a fixed frequency of 0.1 rad/s. Inset: log–log plot of $\eta$ versus reduced MWNT loading. The solid lines are fits to power law dependences of viscosity on MWNT loading (Eq. (3)).

viscosity versus MWNT loading at 0.1 rad/s is displayed in Fig. 10 with $m_{c,\eta}$ of 0.006 and $\beta_{c,\eta}$ of 1.3. The best fitting for storage modulus versus MWNT loading at 0.158 rad/s is shown in Fig. 11 with $m_{c,G'}$ of 0.005 and $\beta_{c,G'}$ of 1.5. The overall fitting results from power law relations for electrical conductivity ($\sigma$), viscosity ($\eta$) and storage modulus ($G'$) versus MWNT loading ($m$) are listed in Table 2. The rheological percolation thresholds fitted from viscosity at 0.1 rad/s is about 0.6 wt% and from storage modulus at 0.158 and 10 rad/s is about 0.5 wt%.

Kharchenko et al. [3] prepared polypropylene/MWNT nanocomposites using melt blending, and they founded that the percolation thresholds for firmness at 200 °C is in the concentration range 0.25–1 vol%. Pötschke et al. [13] produced polycarbonate/MWNT nanocomposites by melt mixing, and they concluded that the rheological percolation threshold was strongly dependent on the measurement temperature. It changed from about 5–0.5 wt% MWNT by

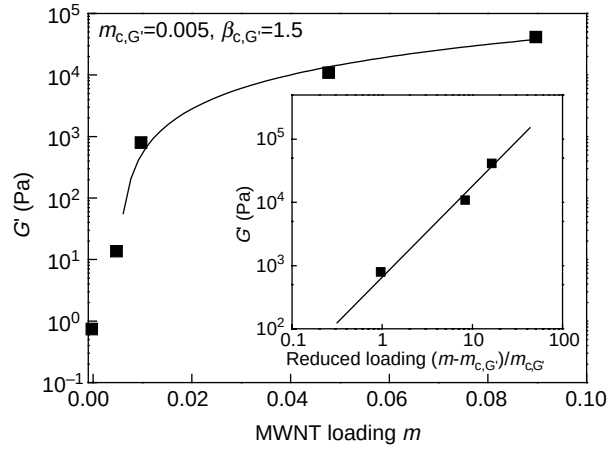


Fig. 11. Storage modulus ($G'$) of PET/MWNT nanocomposites as a function of MWNT loading at a fixed frequency of 0.158 rad/s. Inset: log–log plot of $G'$ versus reduced loading. The solid lines are fits to power law dependences of storage modulus on MWNT loading (Eq. (4)).

Table 2
Fitting results from power law relations of electrical conductivity ($\sigma$), viscosity ($\eta$) and storage modulus ($G'$) versus MWNT loading ($m$)

| Power law relation | $m$ (%) | $\beta$ |
|---|---|---|
| $\sigma \propto (m-m_{c,\sigma})^{\beta_{c,\sigma}}$ | 0.9 | 2.2 |
| $\eta \propto (m-m_{c,\eta})^{\beta_{c,\eta}}$ at 0.1 rad/s | 0.6 | 1.3 |
| $G' \propto (m-m_{c,G'})^{\beta_{c,G'}}$ at 0.158 rad/s | 0.5 | 1.5 |
| $G' \propto (m-m_{c,G'})^{\beta_{c,G'}}$ at 10 rad/s | 0.5 | 1.5 |

increasing the measurement temperature from 170 to 280 °C, respectively. Du et al. [21] prepared PMMA/SWNT nanocomposites via coagulation method, and they pointed out the rheological percolation threshold of these nanocomposites is 0.12 wt%. In the present case of PET/MWNT nanocomposites, the rheological percolation thresholds fitted from viscosity at 0.1 rad/s is about 0.6 wt% and from storage modulus at 0.158 and 10 rad/s at 265 °C is about 0.5 wt%. These values are comparable to previous results on thermoplastics/CNT nanocomposites published by other groups. The low rheological percolation threshold may be attributed the fact that homogeneous dispersion of MWNT in PET matrix and high aspect ratio of MWNT makes it possible to possess percolation threshold at low MWNT loading in nanocomposites.

### 3.4. Comparison between the electrical and rheological percolation thresholds

The percolation threshold of 0.6 wt% (based on viscosity) for rheological property and 0.9 wt% for electrical conductivity obtained from PET/MWNT nanocomposites is one of the lowest values of percolation threshold reported so far in MWNT nanocomposites with thermoplastics. The low percolation threshold results from homogeneous dispersion of MWNT in PET matrix and high aspect ratio of MWNT. Both electrical and rheological properties of PET nanocomposites show similar percolation behaviors, pointing out that both of them are sensitive to interconnectivity of MWNT in PET matrix. In spite of rigidity of carbon nanotubes, their small cross-sectional dimensions and high aspect ratio consent to their fully bending in response to inter-tube interactions and environmental changes [3,40]. As shown above in TEM micrographs (Fig. 2(a) and (b)), MWNT exhibit some degree of waviness or entanglements along axial direction. At loadings greater than that for random close packing of the rigid tubular objects, the bending leads to formation of disordered reticular structure with the substantial mechanical integrity [41]. The presence of nanotube network interpenetrating into PET matrix creates additional large contributions to viscoelasticity of the nanocomposites [3]. When the randomly placed overlapping objects exceeds critical loading of the fillers, known as the percolation threshold, an increase in electrical conductivity and viscosity with several orders of magnitude can be observed.

The coincidence of percolation behavior of electrical and rheological properties has also been observed in other polymer–CNT systems such as polypropylene/MWNT [3,4], polycarbonate/MWNT [12,13], and PMMA/SWNT [21].

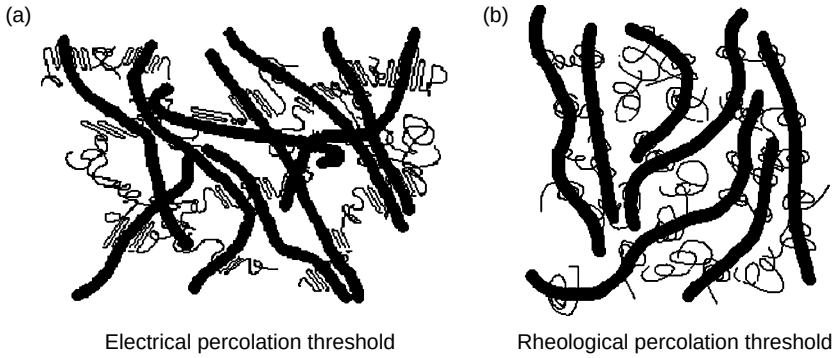


Fig. 12. Illustration of electrical percolation threshold (a) and rheological percolation threshold (b) in PET/MWNT nanocomposites. The thick lines stand for MWNT, and the thin ones for PET chains.

The difference between the electrical and rheological percolation thresholds is mainly attributed to different stages of nanotube network required [13,21]. It is assumed that when nanotubes reach the electrical percolation threshold in polymeric matrix, they need not always physically touch each other, and they can be just close enough to allow the hopping/tunneling processes, as illustrated in Fig. 12(a). The electron hopping/tunneling mechanism requires tube-tube distance to be less than 5 nm to be electrically conductive. Because the etching experiments reveal that the coating of PET chains onto MWNT is actually semi-crystalline, the PET chains attached to MWNT are represented as chain folded chains. Whereas, when the gap between two nanotubes is smaller than the radius of gyration of a polymer chain in molten state, generally about dozens of nanometers, the nanotubes can be linked by random coils of polymer chains and impede the polymer chain mobility, as illustrated in Fig. 12(b). Thus, the inter-tube distance required for rheological percolation threshold is longer than that for electrical percolation threshold, meaning that fewer nanotubes are needed to approach to rheological percolation threshold than that for electrical percolation threshold. Meanwhile, the nanotubes with defects and a number of less conductive nanotubes contribute little to the electrical property of the materials. Therefore, a denser nanotube network is required to reach the electrical percolation threshold than that for the rheological percolation threshold.

## 4. Conclusions

PET/MWNT nanocomposites have first been prepared by means of coagulation. Uniform dispersion of MWNT throughout PET matrix was confirmed by TEM and SEM observations. The encapsulation of MWNT by PET chains was found by quantitative comparison of micrographs of purified MWNT, unetched and etched MWNT encapsulated by PET chains. This encapsulation is considered as evidence of interfacial interaction between MWNT and PET chains. The percolation threshold of 0.9 wt% in MWNT loading for electrical conductivity at room temperature is found. At 1 wt% of MWNT loading, the electrical conductivity level exceeds antistatic criterion of thin films ($1\times10^{-8}$ S/cm). The rheological behaviors of PET nanocomposites were investigated using oscillatory rheometry at temperature of 265 °C. With increasing MWNT loading, the melt behavior transits from liquid-like to solid-like viscoelastic. The rheological percolation threshold fitted from viscosity at 0.1 rad/s is 0.6 wt%, and that fitted from storage modulus at 0.158 rad/s is 0.5 wt%. The low percolation threshold on electrical conductivity and rheology results from homogeneous dispersion of MWNT in PET matrix and high aspect ratio of MWNT. The rheological percolation threshold is less than its electrical conductivity counterpart. This shows that, although both rheological and electrical properties are sensitive to interconnectivity of MWNT, their responses are different, which is mainly attributed to the fact that denser nanotube network is required to allow hopping/tunneling processes of electrons than impede polymer chain mobility.

## Acknowledgements

Z.G. Wang acknowledges the financial support from ‘One Hundred Young Talents’ of Chinese Academy of Sciences and the National Science Foundation of China with grant number NSFC 10590355.

## References

[1] Ijima S. Nature 1991;354(6348):56–8.
[2] Bin Y, Kitanaka M, Zhu D, Matsuo M. Macromolecules 2003;36(16):6213–9.
[3] Kharchenko SB, Douglas JF, Obrzut J, Grulke EA, Migler KB. Nat Mater 2004;3(8):564–8.
[4] Seo MK, Park SJ. Chem Phys Lett 2004;395(1-3):44–8.
[5] Kashiwagi T, Grulke E, Hilding J, Harris R, Awad W, Douglas J. Macromol Rapid Commun 2002;23(13):761–5.
[6] Kashiwagi T, Grulke E, Hilding J, Groth K, Harris R, Butler K, et al. Polymer 2004;45(12):4227–39.
[7] Zhang WD, Shen L, Phang IY, Liu T. Macromolucules 2004;37(2):256–9.
[8] Liu T, Phang IY, Shen L, Chow SY, Zhang WD. Macromolucules 2004;37(19):7214–22.
[9] Sandler JKW, Pegel S, Cadek M, Gojny F, van Es M, Lohmar J, et al. Polymer 2004;45(6):2001–15.
[10] Meincke O, Kaempfer D, Weickmann H, Friedrich C, Vathauer M, Warth H. Polymer 2004;45(3):739–48.
[11] Tang W, Santare MH, Advani SG. Carbon 2003;41(14):2779–85.
[12] Pötschke P, Fornes TD, Paul DR. Polymer 2002;43(11):3247–55.

[13] Pötschke P, Abdel-Goad M, Alig I, Dudkin S, Lellinger D. Polymer 2004; 45(26):8863–70.
[14] Pötschke P, Bhattacharyya AR, Janke A. Carbon 2004;42(5-6):965–9.
[15] Nogales A, Broza G, Roslaniec Z, Schulte K, Sÿics I, Hsiao BS, et al. Macromolecules 2004;37(20):7669–72.
[16] Regev O, Elkati PNB, Loos J, Koning CE. Adv Mater 2004;16(3):248–51.
[17] Martin CA, Sandler JKW, Shaffer MSP, Schwarz MK, Bauhofer W, Schulte K, et al. Compos Sci Technol 2004;64(15):2309–16.
[18] Sandler JKW, Kirk JE, Kinloch IA, Shaffer MSP, Windle AH. Polymer 2003;44(17):5893–9.
[19] Ounaies Z, Parkb C, Wiseb KE, Siochic EJ, Harrisonc JS. Compos Sci Technol 2003;63(11):1637–46.
[20] Du F, Fisher JE, Winey KI. J Polym Sci, Part B: Polym Phys 2003;41(24): 3333–8.
[21] Du F, Scogna RC, Zhou W, Brand S, Fischer JE, Winey KI. Macromolecules 2004;37(24):9048–55.
[22] Smith Jr JG, Connell JW, Delozier DM, Lillehei PT, Watson KA, Lin Y, et al. Polymer 2004;45(3):825–36.
[23] Kao CC, Young RJ. Compos Sci Technol 2004;64(15):2291–5.
[24] Kogonemaru A, Bin Y, Agari Y, Matsuo M. Adv Funct Mater 2004;14(9): 842–50.
[25] Sabba Y, Thomas EL. Macromolecules 2004;37(13):4815–20.
[26] Sen R, Zhao B, Perea D, Itkis ME, Hu H, Love J, et al. Nano Lett 2004; 4(3):459–64.
[27] Levi N, Czerw R, Xing S, Iyer P, Carroll DL. Nano Lett 2004;4(7): 1267–71.
[28] Cadek M, Coleman JN, Ryan KP, Nicolosi V, Bister G, Fonseca A, et al. Nano Lett 2004;4(2):353–6.
[29] Wu M, Shaw LLJ. Power Sources 2004;136(1):37–44.
[30] Saran N, Parikh K, Suh D, Muñoz E, Kolla H, Manohar SK. J Am Chem Soc 2004;126(14):4462–3.
[31] Bahr JL, Yang J, Kosynkin DV, Bronikowski MJ, Smalley RE, Tour JM. J Am Chem Soc 2001;123(27):6536–42.
[32] Chiang IW, Brinson BE, Smalley RE, Margrave JL, Hauge RH. J Phys Chem B 2001;105(6):1157–61.
[33] Niyogi S, Hamon MA, Perea DE, Kang CB, Zhao B, Pal SK, et al. J Phys Chem B 2003;107(34):8799–804.
[34] Fagan SB, Filho AGS, Lima JOG, Filho JM, Ferreira OP, Mazali IO, et al. Nano Lett 2004;4(7):1285–8.
[35] Fisher FT, Bradshaw RD, Brinson LC. Appl Phys Lett 2002;80(24): 4647–9.
[36] Wber M, Kamal MR. Polym Compos 1997;18(6):711–25.
[37] Garboczi EJ, Snyder KA, Douglas JF, Thorpe MF. Phys Rev E 1995; 52(1):819–28.
[38] Mutel AT, Camel MR. In: Utracki LA, editor. Two phase polymer systems. Rheological properties of fibre-reinforced polymer melts, vol. 12. Munich: Carl Hanser; 1991. p. 305–31.
[39] Ray SS, Okamoto M. Prog Polym Sci 2003;28(11):1539–641.
[40] Yakobson BI, Brabec CJ, Bernholc J. Phys Rev Lett 1996;76(14): 2511–4.
[41] Aral BK, Kalyon DM. J Rheol 1997;41(3):599–620.